



**Evaluation of natural radioactivity and its associated health hazard indices of a south Indian river**

Journal:	<i>Radiation Protection Dosimetry</i>
Manuscript ID:	RPD-13-0183.R1
Manuscript Type:	Paper
Subject Index Term:	Natural radiation, Dosimetry: physical basis, Dose equivalent/effective dose etc., Gamma radiation/spectrometry, Radiation risks, Statistical analysis

SCHOLARONE™  
Manuscripts

Review

## Evaluation of natural radioactivity and its associated health hazard indices of a south Indian river

N. Krishnamoorthy <sup>a1, a2\*</sup>, S. Mullainathan <sup>b</sup>, R. Mehra <sup>c</sup>, Marcos A E Chaparro <sup>d</sup>, Mauro A E Chaparro <sup>e</sup>

<sup>a1</sup> Research and Development Centre, Bharathiar University, Coimbatore- 641 046, Tamilnadu, India

<sup>a2</sup> Department of Physics, CSI College of Engineering, Ketti- 643 215, Tamilnadu, India

<sup>b</sup> Department of Physics, AVC College of Engineering, Mayiladuthurai-608 002, Tamilnadu, India

<sup>c</sup> Department of Physics, Dr B R Ambedkar National Institute of Technology, Jalandhar -144 011, India

<sup>d</sup> Instituto de Fisica, Arroyo Seco (UNCPBA), CONICET, Pinto 399, B7000GHG Tandil, Argentina

<sup>e</sup> Instituto Multidisciplinario de Ecosistemas y Desarrollo Sustentable (UNCPBA), CONICET, Pinto 399, B7000GHG Tandil, Argentina

### ABSTRACT

The activity concentrations of the natural radionuclides  $^{226}\text{Ra}$ ,  $^{232}\text{Th}$  and  $^{40}\text{K}$  are measured for sediment samples collected from thirty three different locations along the Bharathapuzha river basin by using high- resolution gamma-ray spectrometry. The concentrations of natural radionuclides was found to vary from location to location and their mean values are 19.6%, 82.87% and 19.44% higher than the world-wide mean values of  $^{226}\text{Ra}$ ,  $^{232}\text{Th}$  and  $^{40}\text{K}$ , respectively. The value of  $^{232}\text{Th}$  was found to be higher than  $^{226}\text{Ra}$  in 82% of the samples collected for this study. The calculated values of indoor absorbed dose rate ranged between 89.55 nGy/h to 194.24 nGy/h and the overall mean value is 63.2% higher than the recommended safe and criterion limit by UNSCEAR. The internal and external hazard indices ( $H_{\text{in}}$ ,  $H_{\text{ex}}$ ), the representative gamma index and alpha index ( $I_{\gamma}$ ,  $I_{\alpha}$ ), the annual gonad dose equivalent (AGDE) and the excess life-time cancer risk (ELCR) are also calculated and compared with the international recommended values. Multivariate statistical analyses were also carried out to determine the relation between the natural radionuclides and various radiological parameters.

Keywords: Natural radioactivity; hazard indices; frequency distribution; multivariate statistical analyses; Bharathapuzha river sediments

### 1. Introduction

All materials on earth contain various amounts of natural radionuclides. Human beings are continuously exposed to natural background radiation from the earth surface, building materials and recycled industrial waste products <sup>(1, 2)</sup>. The most important for the purpose of radiation protection to gamma radiation are uranium ( $^{238}\text{U}$ ), thorium ( $^{232}\text{Th}$ ) decay chains and the radioactive isotope of potassium ( $^{40}\text{K}$ ) <sup>(3)</sup>. The occurrence of uranium and thorium is only at trace levels but potassium content is about 0.018% of the total amount in the earth crust <sup>(4)</sup>. The contribution from the  $^{238}\text{U}$  and the other  $^{226}\text{Ra}$  precursors are normally ignored because 98.5% of the radiological

effects of the uranium series are produced by radium and its daughter products<sup>(5)</sup>. Since  $^{40}\text{K}$  is a gamma ray emitter in addition to beta decay, it contributes significantly to gamma radiation exposure (about 54 %) in normal background areas<sup>(6)</sup>. The half-life of these ionizing radiations is  $1.248 \times 10^9$  years for  $^{40}\text{K}$ ,  $1.405 \times 10^{10}$  years for  $^{232}\text{Th}$  and  $4.468 \times 10^9$  years for  $^{238}\text{U}$ . The half-lives of these radionuclides are comparable to the age of earth and therefore found in different building materials<sup>(7)</sup>. The primary sources of external exposure in building are the naturally occurring radionuclides present in various building materials. River sediments are one of the most important building materials in India like in other countries of the world. It is of great interest to note that mineral based building materials has the highest concentration of radionuclides<sup>(8)</sup>. River sediments are mineral deposits made up of materials derived from natural materials like rock, soil, biological and anthropogenic inputs that is broken down by the process of weathering and erosion of either igneous or metamorphic rocks which is subsequently transported by water or wind<sup>(9)</sup>. Generally, natural radionuclides in river sediments depend on the geology of their site of origin<sup>(7, 10, 11)</sup>. In an average, people are exposed to about 2.3 mSv/year by such naturally occurring radioactive materials (NORM). Every human spends 80% of his time inside a room (19/24) and 20% of his time outdoors (5/24) in an average every day and they are exposed to radiation from building materials in two ways (i) external radiation due to the presence of primordial radionuclides in building materials, (ii) internal exposure due to radon inhalation<sup>(12)</sup>. Internal exposure arises due to the inhalation of alpha particles emitted from the short-lived radionuclides of radon ( $^{222}\text{Rn}$ : the daughter product of  $^{226}\text{Ra}$ ) and thoron ( $^{220}\text{Rn}$ : the daughter product of  $^{224}\text{Ra}$ ), while the external exposure is due to the gamma radiation from the radionuclides. One of the main contributors to indoor radon concentrations are the materials from which buildings are constructed<sup>(13, 14)</sup>. Radon, a noble gas, can easily diffuse from the surface of the earth and building materials and can be a source of health hazard related to bronchus and lungs<sup>(15, 16)</sup>. Studies on natural radioactivity were carried out in many other South Indian rivers in the past.<sup>(17, 18, 19)</sup>. In order to assess the radiological risk arising from natural radionuclides in river sediments, an attempt has been made for the first time in Bharathapuzha river to study the levels of radiation emitted from them.

## 2. Materials and methods

### 2.1. Geology of the study area

In the southern part of India, Bharathapuzha river which is 209 km long flows through two major economic states (Tamilnadu and Kerala) and three districts (Coimbatore, Palakkad and Malappuram) bounded by  $10^\circ 26'$  and  $11^\circ 13'$  north latitudes and  $75^\circ 53'$  to  $77^\circ 13'$  east longitudes. The river originates at the foot of Anamalai hills in Coimbatore district, Tamilnadu State and flows towards west direction and then discharges into the Arabian sea at Ponnani in Malappuram district, Kerala State. Bharathapuzha river is considered as the Nile of Kerala and is also called as Nila. The major tributaries of Bharathapuzha river are Thuthapuzha, Gayathripuzha, Kalpathipuzha and Kannadipuzha. There are eleven reservoirs in this river and there are still under construction. The Malampuzha dam is one of the largest dam in this river. Some other dams include Walayar, Pothundi, Chulliyar, Meenkara etc. Bharathapuzha river flows through three major physiographic regions: the highlands ( $>75\text{m}$  above MSL), the midlands ( $75 - 8 \text{ m}$  above MSL) and lowlands ( $<8 \text{ m}$  above MSL) which constitutes highly varied geological

formations. The catchment area of this river experiences tropical humid climate with humidity range of 80 – 96 % and the average annual temperature is 22.7 – 32.5° C. The average rainfall of this area is about 280 cm. Every year more than 4000 million cubic meters of water flows from Bharathapuzha to Arabian sea. The river is the most important source of drinking and is used commonly for agriculture and domestic purposes. Domestic and agricultural wastes from the population living along the course of the river pollute it to a greater extent. The sediments of this river are extensively used for construction of buildings by the people of Coimbatore, Palakkad and Malappuram districts.

### *2.2. Sample collection and preparation*

Sediments were collected at each sampling location from the bottom of the river during dry season around March through June, 2012. To avoid contaminations, the collected samples were packed in polythene covers, sealed and labeled. A total of thirty three samples were collected in this study. The distance between each sampling location was about 4 – 5 kms. The map of the sampling locations is shown in Fig. 1. Using a Global Positioning System, the latitude and longitude of the sampling locations was recorded in terms of degree-minutes and seconds. The collected sediment samples were transported to the laboratory, pulverized and made to pass through a 2 mm mesh sieve. About 500-600 gms of each sample was crushed into fine powder by using agate mortar and pestle and fine quality of the sample was obtained using a scientific sieve of 150 micron mesh size. The samples were dried in an oven at about 110° C for 24 hours to obtain constant dry weight <sup>(20)</sup> and then were transferred into air-tight PVC containers of uniform sizes (height: 9 cm x diameter: 6.5cm) to its total height to avoid distribution of the gamma radiation emitting decay products. The samples were sealed assuming that <sup>222</sup>Rn and <sup>220</sup>Rn do not escape after packing <sup>(21)</sup> and kept for about 30 days to allow radon and its short-lived progenies to reach radioactive equilibrium before measurement using gamma spectrometry system.

### *2.3. Gamma ray detection system*

The activity concentration of <sup>226</sup>Ra, <sup>232</sup>Th and <sup>40</sup>K in the sediment samples was measured using a co-axial n-type high purity germanium detector (make: EG&G, ORTEC, Oak Ridge, USA). The relative efficiency of the detector is 20% and it has a resolution of 2.0 keV at 1332 keV. To reduce the background level of the system, the detector was maintained in a vertical position and shielded using 4'' lead bricks on all sides of the detector. For the efficiency calibration of the system, the International Atomic Energy Agency (IAEA) standard reference materials RG U-1 (uranium ore), RG Th-1 (thorium ore) and RG K-1 potassium (K<sub>2</sub>SO<sub>4</sub>) are used in the same geometry. The spectrum is calibrated with known sources of radioactivity such as Eu-152 and the efficiency values are plotted against the energy for particular geometry. The samples were placed symmetrically on top of the detector and measured for a counting period of 20 hours. The spectra are analyzed for the peak of radium, thorium daughter products and potassium by subtracting counts due to Compton scattering of higher peaks and other background sources from the total area of the peaks. Gamma transitions of <sup>40</sup>K was determined by measuring the 1461 keV gamma ray emitted during its decay, 186 keV for <sup>226</sup>Ra, 295 and 352 keV for <sup>214</sup>Pb, 609, 1120 and 1764 keV for <sup>214</sup>Bi, 338, 463, 911 and 968 keV for <sup>228</sup>Ac, 727 keV for <sup>212</sup>Bi, 238 keV for <sup>212</sup>Pb are used for the measurement of activity concentrations.

### 3. Results and discussions

#### 3.1. Activity concentration of radionuclides

The activity concentrations of radionuclides in the measured samples are calculated using the equation <sup>(22)</sup>:

$$\text{Activity (Bq kg}^{-1}\text{)} = \frac{\text{CPS} \times 100 \times 100}{\text{B.I.} \times \text{Eff}} \pm \frac{\text{CPS}_{\text{error}} \times 100 \times 100}{\text{B.I.} \times 100} \quad (1)$$

where,

CPS = Net count rate per second

B. I. = Branching Intensity, and

Eff = Efficiency of the detector.

The activity concentrations of the detected radionuclides <sup>226</sup>Ra, <sup>232</sup>Th and <sup>40</sup>K for all the thirty three sediments are presented in Fig. 2. The activity concentration ranges for <sup>226</sup>Ra, <sup>232</sup>Th and <sup>40</sup>K are 21.21 Bq/kg to 66.03 Bq/kg, 33.49 Bq/kg to 93.1 Bq/kg and 232.25 Bq/kg to 899.66 Bq/kg, respectively (Table 1). Average concentration of <sup>226</sup>Ra, <sup>232</sup>Th and <sup>40</sup>K were 41.86 Bq/kg, 54.86 Bq/kg and 477.75 Bq/kg, respectively. These values are 19.6%, 82.87% and 19.44% higher than the recommended world average values for <sup>226</sup>Ra, <sup>232</sup>Th and <sup>40</sup>K, respectively (Fig. 3). The world average value is 35 Bq/kg for <sup>226</sup>Ra, 30 Bq/kg for <sup>232</sup>Th and 400 Bq/kg for <sup>40</sup>K <sup>(3)</sup>. The frequency distribution (in percent) of <sup>226</sup>Ra and <sup>232</sup>Th activity concentrations for all the thirty three sediment samples is presented in Fig. 4. It is interesting to note that about 63% (21 samples) of the activity concentration of <sup>226</sup>Ra were greater than the worldwide mean of 35 Bq/kg. The highest percentage (27%) is due to the activity concentration ranging from 40 to 50 Bq/kg. For <sup>232</sup>Th all the samples (100%) are higher than the worldwide mean of 30 Bq/kg. The highest percentage (18%) is due to the activity concentration from 35 to 40 Bq/kg (6 samples). For <sup>40</sup>K, about 42% of the distributed frequency is below the recommended mean value of 400 Bq/kg and the remaining 58% are above this limit. The activity concentrations was found to vary from one location to the other due to the fact that the river bottom reveals great changes in chemical, mineralogical and the nature of the environment. Increasing activity concentrations may be due to the reason that the radioactive materials passing through clay soil will be removed and held by the clay particles during the horizontal transport of water masses <sup>(23)</sup>. The enhanced concentration of <sup>226</sup>Ra in many locations may be due to the oxidizing condition favoring the formation of UO<sub>2</sub><sup>2+</sup> relative to U (IV) which is highly soluble and has great mobility in almost all environments <sup>(24)</sup>. The lowest concentrations of <sup>232</sup>Th and <sup>40</sup>K may be due to the sandy nature of the sediment whereas the higher concentrations may be due to the high clay content in sediments.

#### 3.2. Environmental impact calculation of the radionuclides

To determine the safety and health status of a person when exposed to the environment, several methods are used to calculate the environmental impacts of natural radionuclides. In the present study, the impacts are evaluated in terms of indoor gamma dose rate, external and internal hazard indices, gamma ray representative level index and alpha index, annual gonad dose equivalent and excess life time cancer risk.

### 3.2.1. Indoor gamma dose rate ( $D_{IN}$ )

When sediments are used as building materials, the indoor gamma dose rate due to the emissions of gamma rays from natural radionuclides  $^{226}\text{Ra}$ ,  $^{232}\text{Th}$  and  $^{40}\text{K}$  inside a standard room of dimensions  $4\text{ m} \times 5\text{ m} \times 2.8\text{ m}$  and following the assumption that the wall thickness is 20 cm and the density of the aggregates is  $2.35 \times 10^3\text{ kg/m}^3$  was calculated using the given formula<sup>(25, 26)</sup>:

$$D_{IN}(\text{nGy/h}) = 0.92 C_{Ra} + 1.1 C_{Th} + 0.080 C_K \quad (2)$$

where,  $C_{Ra}$ ,  $C_{Th}$  and  $C_K$  are the activity concentrations of  $^{226}\text{Ra}$ ,  $^{232}\text{Th}$  and  $^{40}\text{K}$  in Bq/kg, respectively. The calculated indoor gamma dose rate for the 33 samples is shown in Table 2. The calculated minimum and maximum values are 89.55 nGy/h and 194.24 nGy/h, respectively, with a mean value of 137.07 nGy/h. This mean value is 1.63 folds (63.2%) higher than the worldwide mean value (84 nGy/h)<sup>(3)</sup> and is summarized in Table 3. From the calculated  $D_{IN}$  values, it is observed that all the samples exceed the worldwide mean value. Sediment samples with much higher  $D_{IN}$  values may cause radiation hazards and hence must be avoided for construction purposes.

### 3.2.2. External and internal hazard indices ( $H_{ex}$ and $H_{in}$ )

The external hazard index  $H_{ex}$  is an important parameter to evaluate the radiation dose expected to be delivered externally if these materials are used for construction of buildings. This index value must be less than unity for the radiation hazard to be negligible<sup>(27)</sup>:

$$H_{ex} = \frac{C_{Ra}}{370} + \frac{C_{Th}}{259} + \frac{C_K}{4810} \leq 1 \quad (3)$$

where,  $C_{Ra}$ ,  $C_{Th}$  and  $C_K$  are the activity concentrations of  $^{226}\text{Ra}$ ,  $^{232}\text{Th}$  and  $^{40}\text{K}$  in Bq kg<sup>-1</sup>, respectively.

The internal hazard index  $H_{in}$  is used to reduce the internal exposure to  $^{222}\text{Rn}$  and its radioactive progeny. For safety measurements in the usage of materials for building constructions, it should be noted that  $H_{in} \leq 1$ <sup>(28)</sup>. The internal hazard index due to gamma radiation is calculated by the following equation<sup>(27)</sup>:

$$H_{in} = \frac{C_{Ra}}{185} + \frac{C_{Th}}{259} + \frac{C_K}{4810} \leq 1 \quad (4)$$

where,  $C_{Ra}$ ,  $C_{Th}$  and  $C_K$  are the activity concentrations of  $^{226}\text{Ra}$ ,  $^{232}\text{Th}$  and  $^{40}\text{K}$  in Bq kg<sup>-1</sup>, respectively. The calculated external hazard values are between 0.28 and 0.62 with an average value of 0.42, and the internal hazard values are between 0.35 and 0.80 with an average value 0.54. The values of  $H_{ex}$  and  $H_{in}$  for all the samples are less than unity (Table 2) which shows that there is only a little risk of hazards to people using the sediments. These values are about 58% and 46% lower than the worldwide mean values for  $H_{ex}$  and  $H_{in}$ , respectively and are presented in Table 3.

### 3.3.3. Gamma ray representative level index ( $I_\gamma$ ) and alpha index ( $I_\alpha$ )

The gamma ray representative index is used as a tool to estimate the radiation hazards in building materials associated with natural radionuclides. It is defined by the following equation<sup>(29)</sup>:

$$I_{\gamma} = \frac{C_{Ra}}{150} + \frac{C_{Th}}{100} + \frac{C_K}{1500} \quad (5)$$

where,  $C_{Ra}$ ,  $C_{Th}$  and  $C_K$  are the activity concentrations of  $^{226}\text{Ra}$ ,  $^{232}\text{Th}$  and  $^{40}\text{K}$  in  $\text{Bq kg}^{-1}$ , respectively. For building materials, the European Commission (EC) <sup>(26)</sup> has introduced two criteria, an exemption criterion of  $0.3 \text{ mSv y}^{-1}$ , and an upper limit of  $1 \text{ mSv y}^{-1}$ . For building materials like sediment (sand) which are used in bulk quantity, an exemption level of  $0.3 \text{ mSv y}^{-1}$  is considered and the maximum value of  $I_{\gamma}$  should be below 0.5, but if the upper level of  $1 \text{ mSv y}^{-1}$  is considered, then  $I_{\gamma}$  should be less than 1. Materials with  $I_{\gamma} \leq 3$  should be avoided for construction purpose, since these values correspond to dose rates higher than  $1 \text{ mSv/y}$  <sup>(26)</sup>, which is the highest value of dose rate in air recommended for population <sup>(30)</sup>. Among the 33 samples, 21 samples (64%) have  $I_{\gamma} \geq 1$ , 12 samples (34%) are between 0.74 and 0.99 (Table 2). The calculated values of  $I_{\gamma}$  are between 0.74 and 1.63 with an average value of 1.15. Here, the average value of  $I_{\gamma}$  is 2.3 times (65%) higher than the recommended maximum value of 0.5 for materials used in bulk and 1.15 times (15%) higher than the threshold value of 1 (Table 3). It must be taken into account that for all the 33 samples  $I_{\gamma}$  is greater than 0.5, which implies an exposure level greater than  $0.3 \text{ mSv per annum}$ . Higher values of  $I_{\gamma}$  may be due to the higher concentration of radionuclides. However,  $I_{\gamma} < 1$  can be safely used for construction of buildings when the upper limit is taken into consideration.

From the radon inhalation which originates from building materials, the excess alpha radiation is calculated using the following relation <sup>(31, 32)</sup>:

$$I_{\alpha} = \frac{C_{Ra}}{200} \text{ (nGy/h)} \quad (6)$$

where,  $C_{Ra}$  is the activity concentration of  $^{226}\text{Ra}$ . The recommended exemption and upper level of  $^{226}\text{Ra}$  activity concentrations in building materials are 100 and 200  $\text{Bq / kg}$ , respectively, as suggested by <sup>(33)</sup>. These considerations are reflected in the alpha index. The recommended upper limit concentration of  $^{226}\text{Ra}$  is 200  $\text{Bq/kg}$ , for which  $I_{\alpha} = 1$ . The calculated  $I_{\alpha}$  value are between 0.11 and 0.33 with a mean value of 0.21 which is 79% less than the world recommended mean value (Table 3).

### 3.3.4. Annual gonad dose equivalent (AGDE)

The activity bone marrow and the bone surface cells are considered as the organs of interest by UNSCEAR (1988) <sup>(34)</sup>. Therefore, the AGDE for people living inside a building due to the specific activities of  $^{226}\text{Ra}$ ,  $^{232}\text{Th}$  and  $^{40}\text{K}$  present in building materials is calculated using the following formula <sup>(35, 36)</sup>:

$$\text{AGDE } (\mu\text{Sv/y}) = 3.09 C_{Ra} + 4.18 C_{Th} + 0.314 C_K \quad (7)$$

where,  $C_{Ra}$ ,  $C_{Th}$  and  $C_K$  are the activity concentrations of  $^{226}\text{Ra}$ ,  $^{232}\text{Th}$  and  $^{40}\text{K}$  in  $\text{Bq / kg}$ , respectively. The obtained values of AGDE are presented in Table 2. The values ranged between 330  $\mu\text{Sv/y}$  and 716.71  $\mu\text{Sv/y}$  and the average value was found to be 508.66  $\mu\text{Sv/y}$  which is 1.7 times (70%) higher than the world recommended value <sup>(37)</sup> (Table 3).



### 3.3.5. Excess life time cancer risk (ELCR)

Excess Lifetime Cancer Risk (ELCR) is calculated using below equation:

$$\text{ELCR} = \text{AEDE} \times \text{DL} \times \text{RF} \quad (8)$$

where, AEDE, DL and RF are the total annual effective dose equivalent (in  $\mu\text{Sv/y}$ ), duration of life (70 years) and risk factor (S/v), fatal cancer risk per sievert. For stochastic effects, ICRP 60 uses values of 0.05 for the public<sup>(38)</sup>. The calculated values of AEDE for all the sediment samples are clearly presented in Krishnamoorthy et al. (2013)<sup>(39)</sup>. The ELCR values were found to be higher near the origin of the river (Table 2). This may be due to the higher activity concentration in the sampling locations. From Table 3, the calculated ELCR values ranged from 0.21 to  $0.46 \times 10^{-3}$  with an average of  $0.32 \times 10^{-3}$  which is 1.10 (10.3%) times higher than the worldwide recommended value of  $0.29 \times 10^{-3}$ <sup>(3)</sup>.

### 3.3.6. Summary of radiological parameters

The summary of the calculated values of radiological parameters are presented in Table 3. It is clearly pointed that indoor gamma dose rate ( $D_{\text{IN}}$ ), gamma ray representative level index ( $I_{\gamma}$ ), annual gonad dose equivalent (AGDE) and excess life time cancer risk (ELCR) are higher than the world-wide mean value by 63.2 %, 15%, 70% and 10.34%, respectively. Radiological parameters like external and internal hazard indices ( $H_{\text{ex}}$  and  $H_{\text{in}}$ ) and alpha index ( $I_{\alpha}$ ) are less than the world-wide mean value by 58%, 46% and 79%, respectively. The graphical representation of the increase / decrease percentage with the world-wide mean is shown in Fig.5.

### 3.3.7. $^{226}\text{Ra}$ , $^{232}\text{Th}$ and $^{40}\text{K}$ activity concentration ratios

The distributions of activity concentration ratios of Bharathapuzha river sediments are presented in Table 4. The analyses of Ra/Th activity ratio concentrations give an exposure that the mean value of  $^{226}\text{Ra}$  activity concentration is 0.52 times lower than the mean value  $^{232}\text{Th}$  activity concentration. The highest value and the lowest value of Ra/Th ratio are 1.19 and 0.38, respectively. On the other hand, the highest value and the lowest value of Th/Ra ratio are 2.64 and 0.84, respectively. The mean value of Th/Ra (1.34) is 1.63 times higher than the mean value of Ra/Th (0.82). This indicates absence of loamy sediments and higher  $^{232}\text{Th}$  activity concentration than  $^{226}\text{Ra}$  along the river basin. From the Ra/K, the values were in the range 0.02 to 0.19 with a mean value of 0.10. Result obtained for Th/K ranges between 0.05 to 0.27 with a mean value 0.13. Here, the highest value of Ra/K is 9.5 times greater than the lowest value, whereas, for Th/K it is 5.4 times greater. Moreover, the Th/Ra values ranging between 0.3 – 2 indicates the presence of zircon in the sediment samples<sup>(40)</sup>.

### 3.3.8. Statistical analysis

Multivariate statistical analyses were performed using the R free software (R version 2.15.0 2012)<sup>(41)</sup>. Pearson's correlation analyses were carried out to determine the interrelation between the natural radionuclides and radiological hazard parameters. The obtained correlation coefficients are presented in Table 5. From the earlier



stated observations<sup>(42, 43)</sup>, it is reported that  $^{238}\text{U}$  series and  $^{232}\text{Th}$  series are usually found together in nature and good correlation between them is indicative of common sources which in general, associated to a mineralogical component. The relative distribution of  $^{226}\text{Ra}$  is positively correlated with  $^{232}\text{Th}$  ( $R = 0.522$ ) and poor correlation was observed between  $^{232}\text{Th}$  and  $^{40}\text{K}$ . Moreover,  $^{226}\text{Ra}$  and  $^{40}\text{K}$  are negatively correlated and this may be due to sediment process that greatly affects the mobility of the radionuclides<sup>(44)</sup>. The activity concentration of  $^{232}\text{Th}$  is positively correlated with all the hazard parameters discussed in the present study. This may be to the rich content of  $^{232}\text{Th}$  which plays an important role in determining the hazard nature in the river sediment. Also, good correlations among most of the hazard parameters were noticed and are indicated with bold values (Table 5).

The fuzzy c-means clustering (FCC) was studied. Thirty three ( $n=33$ ) samples were used for this investigation. For the analyses, seven radioactivity variables were included in the data set. The statistical studies were accomplished in order to get a description of the activity concentration along the river. The FCC method allows us to get a partition (fuzzy clustering) using these variables. According to the normalized Dunn's index<sup>(45)</sup>, the high value (0.72) indicates, or tends, to a near-crisp clustering (values close to 1). Each group is characterized by three centroids that are summarized in Table 6. From these values it is possible to distinguish groups with different activity influences, high (Group 1), moderate (Group 2) and low (Group 3). There are some samples (locations) with behavior not clearly defined (belonging to one group), i.e. samples 1 and 9 belong to Groups 1 and 2. On the other hand, samples 22, 33, 18, 30, 7 and 15 belong to Groups 2 and 3 (see the membership values). It is worth of mentioning that there are not samples belonging to Groups 1 and 3 (Table 7). These groups can be observed in the graphic representation of principal coordinates: PC1 and PC2 (Fig. 6). This representation used a Euclidean distance.

## Conclusion

The average activity concentrations of Bharathapuzha river sediments are 19.6%, 82.87% and 19.44% higher than the world average values for  $^{226}\text{Ra}$ ,  $^{232}\text{Th}$  and  $^{40}\text{K}$ , respectively. From the frequency distribution, 100% of activity concentration for  $^{232}\text{Th}$  is greater than the recommended mean value. The calculated average values of radiological hazard parameters such as indoor gamma dose rate ( $D_{\text{IN}}$ ), Gamma ray representative level index ( $I_{\gamma}$ ) Annual gonad dose equivalent (AGDE) and Excess life time cancer risk (ELCR) are 63.2%, 15%, 70% and 10.34% higher than the recommended level while the other calculated hazard parameters are within the criterion limit suggested by UNSCEAR. The mean Th/Ra activity concentration ratio is 1.63 times greater than that of Ra/Th which may be due the high content of monazite in the study area. Positive and high correlations were observed between hazard parameters and  $^{232}\text{Th}$  than those of  $^{226}\text{Ra}$  and  $^{40}\text{K}$ . This may be due to excess activity concentration of  $^{232}\text{Th}$  in all sampling locations. Using the multivariate statistical analysis group classification was also carried out to classify the risk nature of sediments. From the reported data sediments samples collected from Group 1 locations (Location Nos. 1, 4, 10, 25, 28, 31 and 32) shows excess exposure for the inhabitants and could pose significant radiological threat to the population. Therefore, considering the various factors which affect the health of human beings residing along the Bharathapuzha river basin, sediment samples collected from Group 3 locations can be

extensively used for construction of dwellings whereas sediments belonging to Group 2 can be safely used in small quantities.

### Acknowledgement

The authors are grateful to the University and officials of Health Physics Laboratory of Inter University Accelerator Centre, New Delhi for their support in providing the necessary equipments for gamma-ray spectrometry.

### References

1. NCRP. Natural background radiation in the United States. National Council on Radiation and Measurements, Report No.45, Washington, DC. (1975).
2. Gibson, J. A. B., Thompson, I. M. G., and Spiers, F. W. A guide to the measurement of environmental gamma radiation. National Physical Laboratory, London. (1993).
3. UNSCEAR. United Nations Scientific Committee on the effect of atomic radiation. Sources and effects of ionizing radiation. Report to General Assembly, with scientific annexes, United Nations, New York (2000).
4. Mujahid, S. A., Rahim, A., Hussain, S. and Farooq. Measurements of natural radioactivity and radon exhalation rates from different brands of cement used in Pakistan. Radiat. Prot. Dosim. 130(2), 206–212 (2008).
5. Zastawny, A., Kwasniewicz, E. and Rabsztyn, B. Measurement of the  $^{232}\text{Th}$ ,  $^{238}\text{U}$  and  $^{40}\text{K}$  concentration in some samples of ashes from power stations in Poland. Nukleonika. 24, 535. (1979).
6. Xinwei, L., Lingqing, W., Xiaodan, J., Leipeng, Y. and Gelian D. Specific activity and hazards of Archeozoic-Cambrian rock samples collected from the Weibei area of Shaanxi, China. Radiat. Prot. Dosimetry. 118 (3), 352-359 (2006).
7. Tzortzis, M., Tsertos, H., Christofider, S. and Christodoulides, G. Gamma-ray measurements of naturally occurring radioactive samples from Cyprus characteristic geological rocks. Radiat. Meas 32, 221-229 (2003).
8. Turtiainen, T., Salahel-Din, K., Klemola, S and Sihvonen, A. P. Collective effective dose by the population of Egypt from building materials. J. Radiol. Prot. 28 (2), 223-232 (2008).

9. Veiga, R., Sanches, N., Anjos, R. M., Macario, K., Bastos, J., Iguatemya, M., Aguiar, J. G., Santos, A. M. A., Mosquera, B., Carvalho C., Baptista Filho M. and Umisedo N.K. Measurement of Natural Radioactivity in Brazilian Beach Sands. *Rad. Meas.* 4, 189 – 196 (2006).
10. Mirza, N. M., Ali. B., Mirza, S. M., Tufail, M. and Ahmad, N. A shape and mesh adaptive computational methodology for gamma ray dose from volumetric sources. *Radiat. Prot. Dosim.* 38 (4), 307-314 (1991).
11. Florou, H. and Kritidis, P. Gamma radiation measurements and dose rate in the coastal areas of volcanic island, Aegean sea, Greece. *Radiat. Prot. Dosim.* 45(1/4), 277-279 (1992).
12. Ngachin, M., Garavaglia, M., Giovani, C., Kwato-Njock, M. G. and Nourredine, A. Assessment of natural radioactivity and associated radiation hazards in some Cameroonian building materials. *Radiat. Meas.* 42, 61-67 (2007).
13. Bossew, P. The radon emanation power of building materials, soils and rocks. *Appl. Radiat. Isot.* 59:389–392 (2003).
14. Denman, A. R. and Phillips, P. S. A review of the cost effectiveness of radon mitigation in domestic properties in Northamptonshire. *J Radiol Prot* 18:119–214 (1998).
15. Stidley, C. and Samet, J. A review of ecologic studies of lung cancer and indoor radon. *Health Phys.* 65, 234 (1993).
16. Lubin, J. H. and BOICE J. D. Estimating Rn-induced Lung Cancer in the United States. *Health Phys.* 57, 417 (1989).
17. Ramasamy, V., Suresh, G., V. Ponnusamy, V. and Meenakshisundaram, V. Investigation on natural radiation level and its hazardous nature of river sediments using  $\gamma$ -ray spectroscopy Radiochemistry. 53, (1), 87-96 (2011).
18. Narayana, Y., Rajashekara, K. M. and Siddappa, K. Natural radioactivity in some major rivers of coastal Karnataka on the southwest coast of India. *J. Environ. Radioact.* 95 (2-3),98-106 (2007).
19. Murugesan, S., Mullainathan, S., and Ramasamy, V. Meenakshisundaram, V. Radioactivity and radiation hazard assessment of Cauvery River, Tamilnadu, India. *Iran. J. Radiat. Res.* 8(4), 211-222 (2011).
20. Benke, R. R. and Kearfott, K. J. Soil sample moisture content as a function of time during oven drying for gamma-ray spectroscopic measurements, *Nucl. Instr. Meth. Phys Res. A* 422, 817– 819(1999).

21. El-Taher, A., Uosif, M. A. M. and Orabi, A. A. Natural radioactivity levels and radiation hazard indices in granite from Aswan to Wadi El-Allaqi southeastern desert, Egypt. *Radiat. Prot. Dosim.* 124 (2), 148-154 (2007).
22. Mehra, R., Singh, S., Singh, K. and Sonkawade, R. G.  $^{226}\text{Ra}$ ,  $^{232}\text{Th}$  and  $^{40}\text{K}$  analysis in soil samples from some areas of Malwa region, Punjab, India using gamma ray spectrometry. *Environ. Monit. Assess.* 134, 333-342 (2007).
23. Saad, H. R. and Al-Azmi, D. Radioactivity concentrations in sediments and their correlation to the coastal structure in Kuwait. *Appl. Radiat. Isot.* 26, 991-997 (2002).
24. Powell, B. A., Hughes, L. D., Soreefan, M. A., Deborah Falta, Michael Wall. and Devol, T. A. Elevated concentrations of primordial radionuclides in sediments from the Reedy river and surrounding creeks in Simpsonville, South Carolina. *J. Environ. Radioact.* 94, 121-128 (2007).
25. Turhan, S. and Gunduz, Lu. Determination of specific activity of  $^{226}\text{Ra}$ ,  $^{232}\text{Th}$  and  $^{40}\text{K}$  for assessment of radiation hazards from Turkish pumice samples. *J. Environ. Radioact.* DOI: 10.1016/j.jenvrad.2007.08.022. (2007).
26. European Commission (EC). Radiological Protection Principles Concerning the Natural Radioactivity of Building Materials. Radiation Protection Report No. 112. Directorate-General for Environment, Nuclear Safety and Civil Protection. (1999).
27. Beretka, J. and Mathew, P. Natural radioactivity of Australian building materials, industrial waste and by-products. *Health Phys.* 48, 87-95 (1985).
28. Iqbal, M., Tufail, M. and Mirza, M. Measurement of natural radioactivity in marble found in Pakistan using a NaI (TI) gamma-ray spectrometer. *J. Environ. Radioact.* 51, 255-265 (2000).
29. Mantazul, I., Chowdhury, M. N., Alam, S. K. and Hazari, S. Distribution of radionuclides in the river sediments and coastal soils of Chittagong, Bangladesh and evaluation of the radiation hazard. *Appl. Radiat. Isot.* 51, 747-755 (1999).
30. UNSCEAR. United Nations Scientific Committee on the Effects of Atomic Radiation, United Nations, New York. (1993).

31. Krieger, V. R. Radioactivity of construction materials. *Betonwerk Fertigteil Tech* 47, 468–473 (1981).
32. Stoulos, S., Manolopoulo, M. and Papastefanou, C. Assessment of natural radiation exposure and radon exhalation from building materials in Greece. *J. Environ. Radioact.* 69:225–240 (2003).
33. ICRP Protection against Rn-222 at home and at work Publication No 65, *Ann. ICRP*, 23 (2) (1994).
34. UNSCEAR, 1988. United Nations Scientific Committee on the Effect of Atomic Radiation. Sources, effects and risk of ionizing radiation, United Nations, New York.
35. Mamont-Ciesla, K., Gwiazdowski, B., Biernacka, M. and Zak, A. Radioactivity of building materials in Poland. In: Vohra G, Pillai KC, Sadavisan S (Eds.). *Natural Radiation Environment*. Halsted Press, New York pp.551 (1982).
36. Arafa, W. Specific activity and hazards of granites samples collected from the eastern desert of Egypt, *J. Environ. Radioact.* 75, 315-327 (2004).
37. Zaidi, J. H., Arif, M., Ahmed, S., Fatima, I. and Qureshi, I. H. Determination of natural radioactivity in building materials used in the Rawalpindi Islamabad area by  $\gamma$ -ray spectrometry and instrumental neutron activation analysis, *Appl. Radiat. Isot.* 51, 559-564 (1999).
38. Taskin, H. M., Karavus, P., Ay, A., Touzogh, S., Hindiroglu and Karaham, G. Radionuclide concentration in soil and lifetime cancer risk due to the gamma radioactivity in Kırklareli, Turkey. *J. Environ. Radioact.* 100, 49-53 (2009).
39. Krishnamoorthy, N., Mullainathan, S., Mehra, R., Marcos, A. E. Chaparro and Mauro, A. E. Chaparro. Radiation impact assessment of naturally occurring radionuclides and magnetic mineral studies of Bharathapuzha river sediments, South India. *Environ. Earth. Sci.* DOI: 10.1007/s12665-013-2751-y. (2013).
40. El-Gamel, A., Nasr, N and El-Taher, A. Study of spatial distribution of natural radioactivity in upper Egypt Nile river sediments. *Radiat. Meas.* 42, 457-465 (2007).
41. R version 2.15.0 (2012-03-30). The R Foundation for Statistical Computing [<http://www.r-project.org/>] ISBN 3- 835 900051-07-0 (2012).

42. Seddeek, M. K., Badran, H. M., Sharshar, T. and Elnimr, T. Characteristics, spatial distribution and vertical profile of gamma-ray emitting radionuclides in the coastal environment of North Sinai. *J. Environ. Radioact.* 84, 21-50 (2005).
43. Ligeró, R. A., Vidal, J., Melendez, M. J., Hamani, M. and Casas-Ruiz, M. Sedimentology models from activity concentration measurements: application to the “Bay of Cadiz” Natural Park (SW Spain). *J. Environ. Radioact.* 100, 203-208 (2009).
44. Al-Hamarneh, I. F. and Awadallah, M. I. Soil radioactivity levels and radiation hazard assessment in the Highlands of northern Jordan. *Radiat. Meas.* 44, 102-110 (2009).
45. Dunn JC A fuzzy relative of the ISODATA process and its use in detecting compact well-separated clusters. *J. Cybernetics* 3, 32–57 (1973).

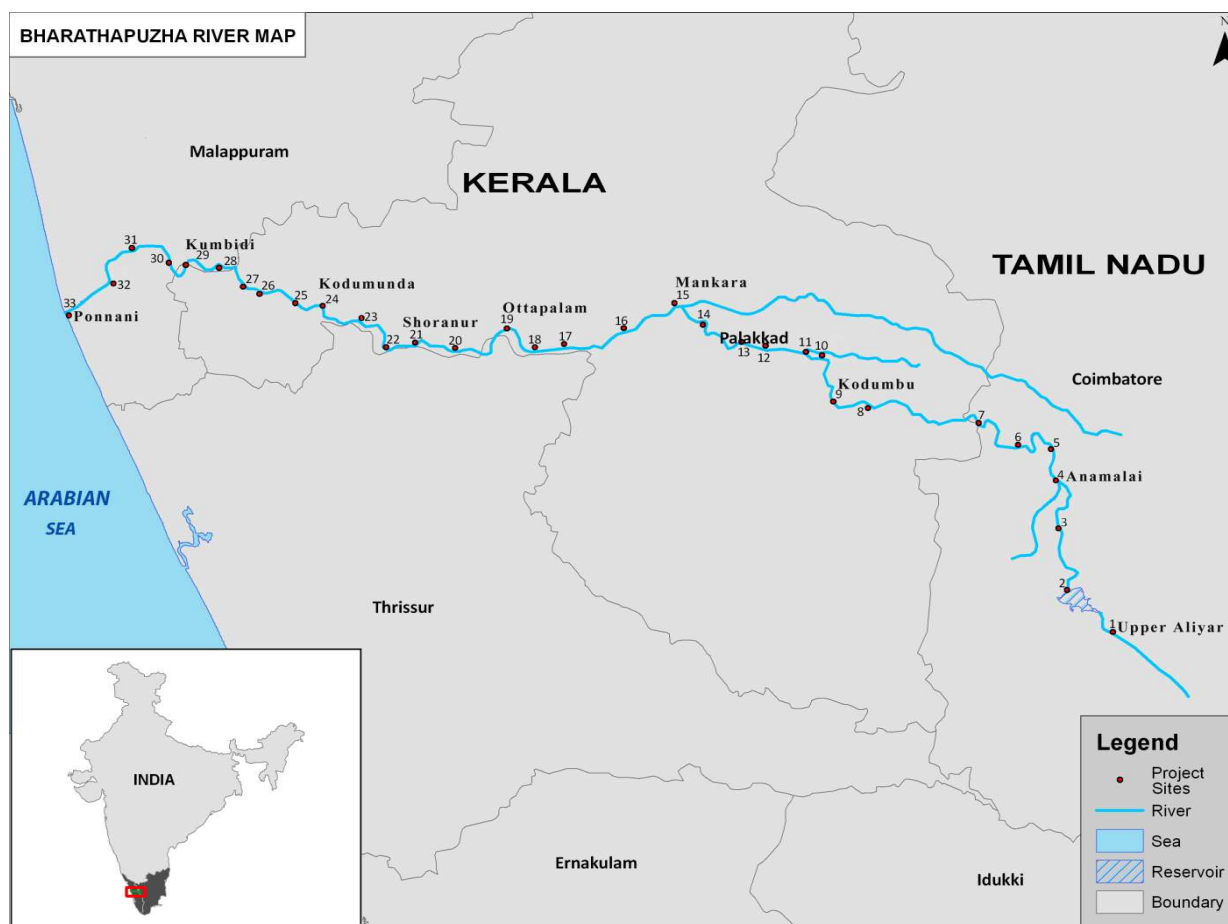


Fig. 1. Map of sampling locations.

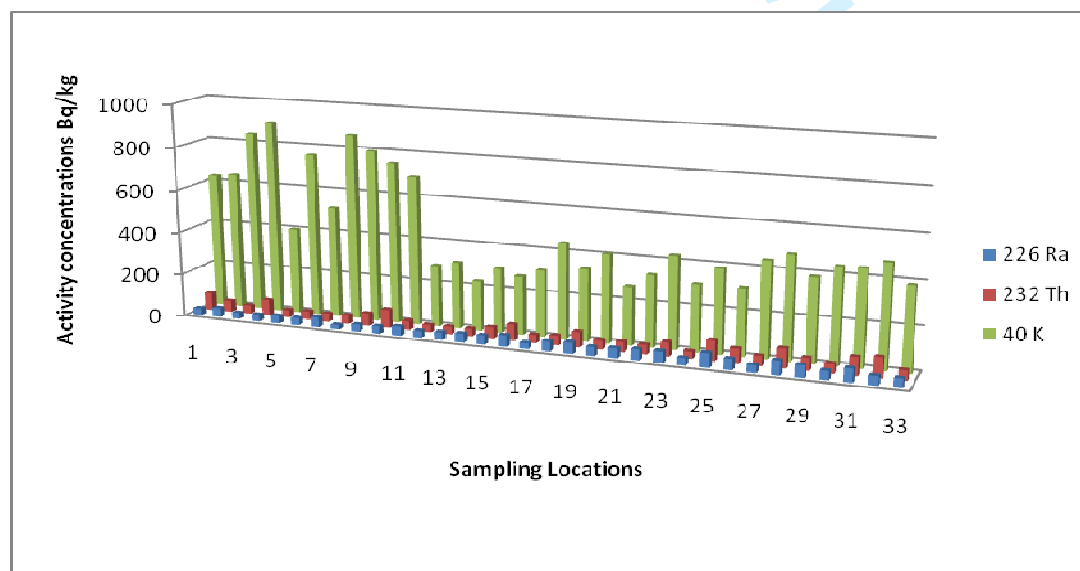


Fig. 2. Activity concentrations of  $^{226}\text{Ra}$ ,  $^{232}\text{Th}$  and  $^{40}\text{K}$  in river sediments along the sampling locations.



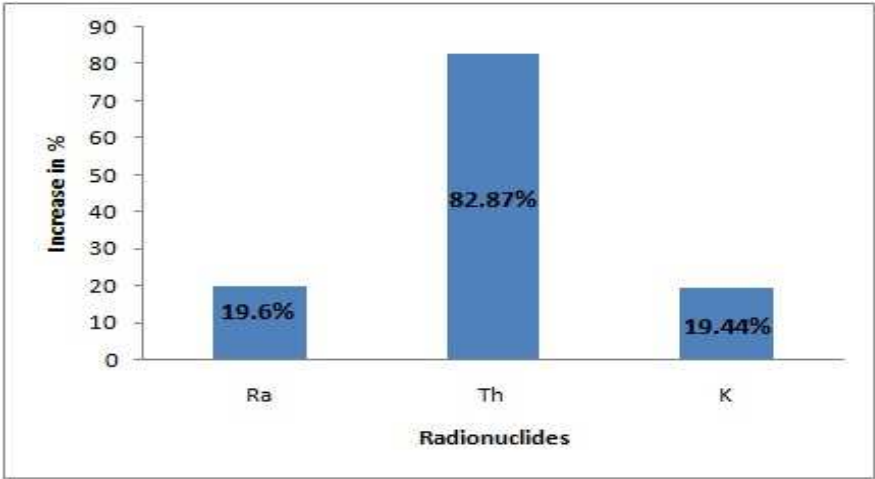
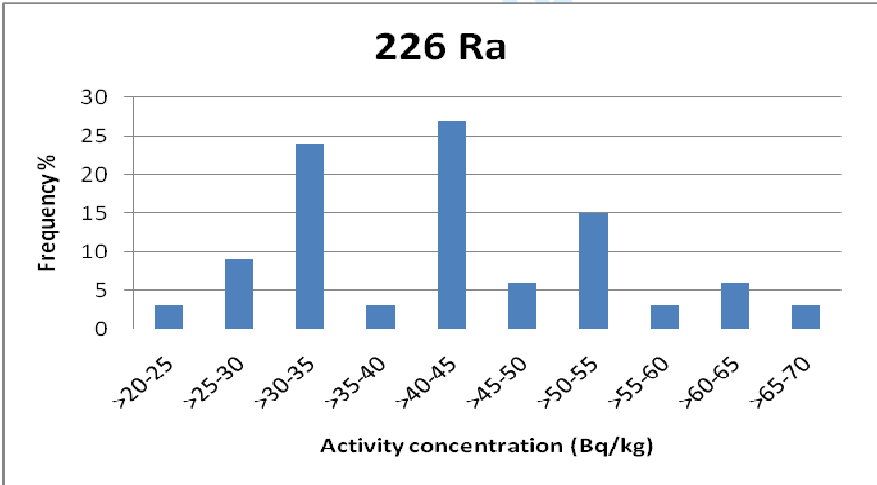


Fig. 3. Increase of natural radionuclides (Bq/kg) in % compared with worldwide mean values



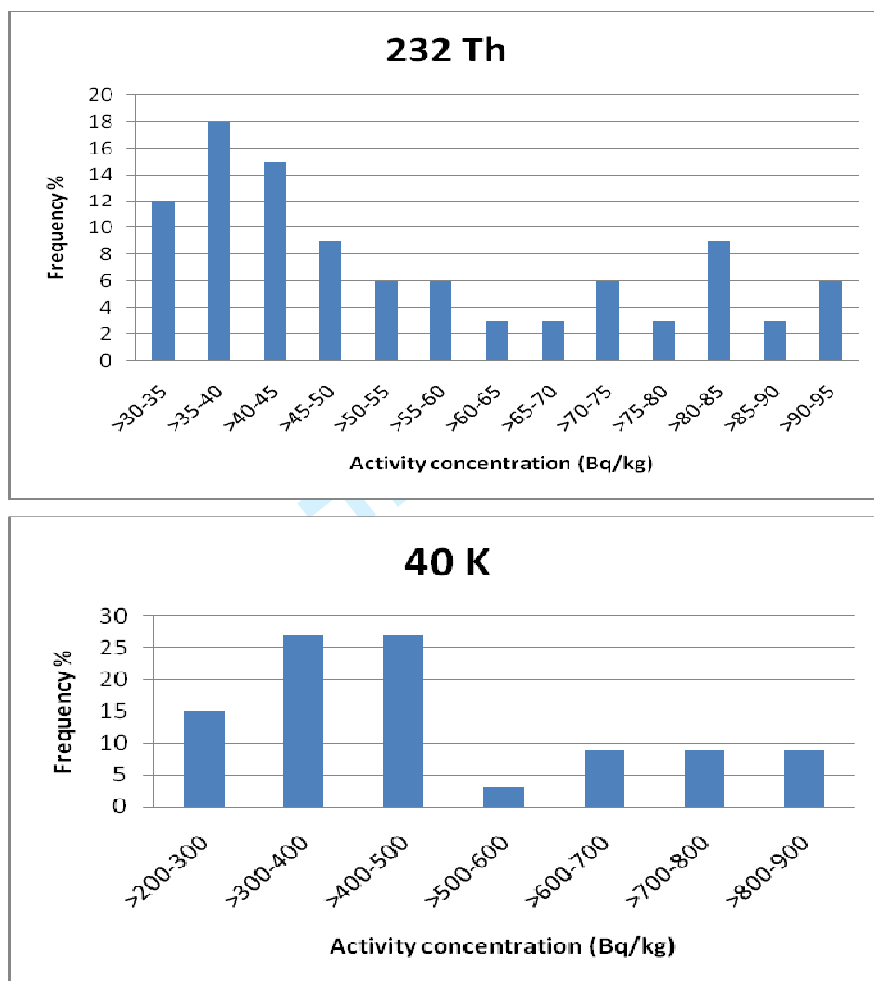


Fig. 4. Frequency distribution of  $^{226}\text{Ra}$ ,  $^{232}\text{Th}$  and  $^{40}\text{K}$  activity concentrations measured in the Bharathapuzha river sediment samples

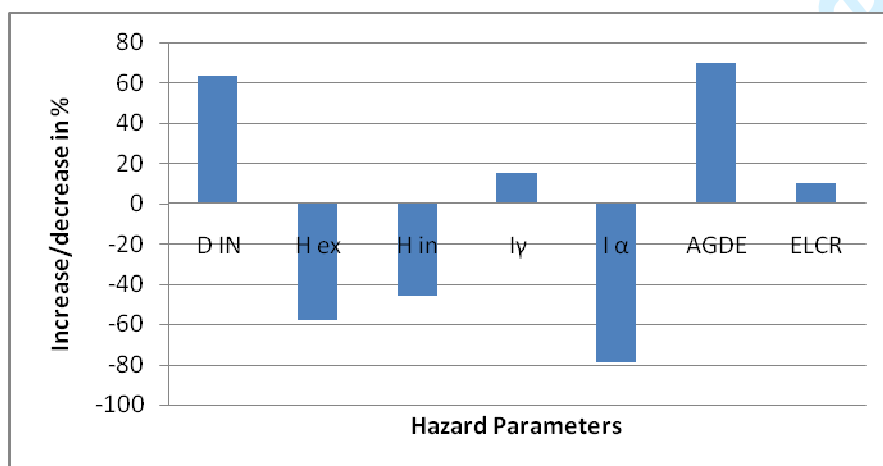


Fig. 5. Increase/decrease % of radiological hazard indices compared with worldwide mean values.

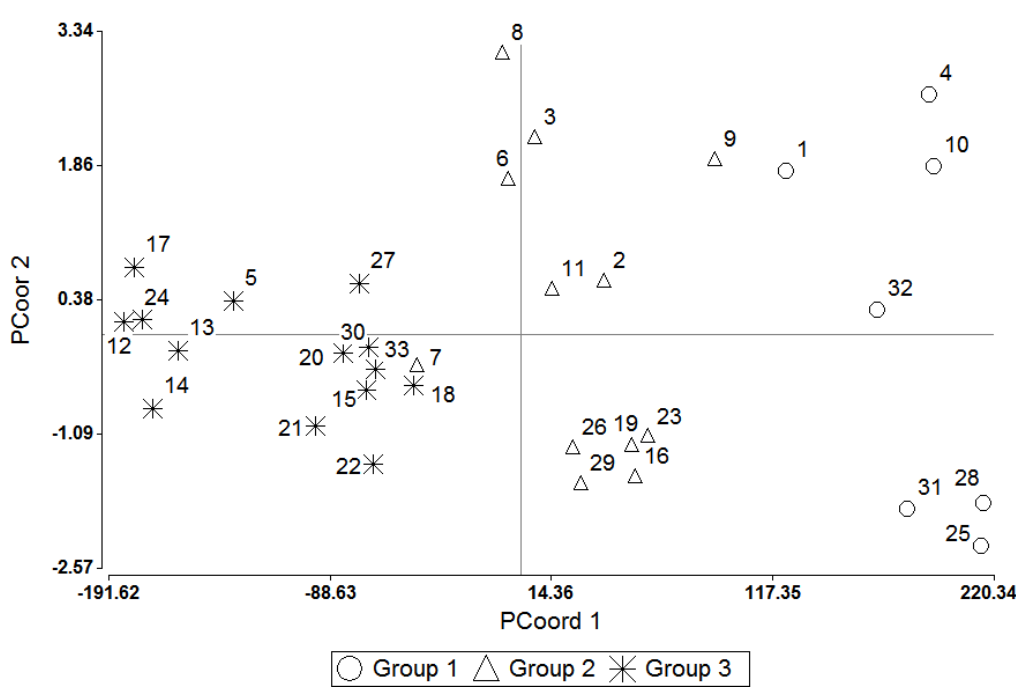


Fig.6. FCC classification, the obtained groups are represented in the coordinate plane (PC 1 and PC 2).

Table 1.

Summary of activity concentrations of <sup>226</sup>Ra, <sup>232</sup>Th and <sup>40</sup>K in sediment samples.

Radionuclides	Minimum (Bq/kg)	Maximum (Bq/kg)	Mean (Bq/kg)	Standard Deviation	Median	World Average (Bq/kg)	Increase/Decrease of mean with world average in %
<sup>226</sup> Ra	21.21	66.03	41.86	10.73	40.99	35	(+) 19.6
<sup>232</sup> Th	33.49	93.1	54.86	19.27	45.96	30	(+) 82.87
<sup>40</sup> K	232.25	899.66	477.75	192.62	428.03	400	(+) 19.44

(+): Increase in value

Table 2.

Indoor dose rate ( $D_{IN}$ ) and radiological hazard parameters ( $H_{ex}$ ,  $H_{in}$ ,  $I_{\gamma}$ ,  $I_{\alpha}$ , AGED and ELCR) in sediment samples.

Sample Location Number	$D_{IN}$ (nGy/h)	$H_{ex}$	$H_{in}$	$I_{\alpha}$	$I_{\gamma}$	AGED ( $\mu$ Sv/y)	ELCR ( $\times 10^{-3}$ )
1	167.02	0.52	0.61	1.43	0.15	628.59	0.40
2	146.48	0.45	0.56	1.22	0.20	546.41	0.34
3	136.73	0.40	0.48	1.14	0.15	515.81	0.32
4	183.24	0.56	0.64	1.56	0.15	693.02	0.44
5	102.42	0.31	0.40	0.85	0.17	379.42	0.24
6	133.95	0.40	0.48	1.12	0.16	503.54	0.31
7	124.99	0.38	0.50	1.03	0.23	461.78	0.29
8	131.95	0.39	0.45	1.11	0.11	501.43	0.31
9	158.42	0.48	0.57	1.34	0.16	596.65	0.37
10	184.59	0.58	0.67	1.57	0.17	695.05	0.44
11	140.40	0.42	0.54	1.16	0.21	523.15	0.32
12	89.55	0.28	0.36	0.74	0.16	330.00	0.21
13	96.33	0.30	0.39	0.80	0.18	354.37	0.22
14	94.03	0.29	0.40	0.77	0.20	343.18	0.22
15	119.29	0.37	0.49	0.99	0.21	439.23	0.28
16	152.29	0.49	0.63	1.28	0.26	559.96	0.36
17	90.26	0.28	0.35	0.76	0.14	335.01	0.21
18	124.81	0.38	0.50	1.03	0.23	460.25	0.29
19	151.53	0.48	0.62	1.27	0.25	558.44	0.36
20	116.03	0.36	0.47	0.96	0.20	428.53	0.27
21	113.60	0.36	0.48	0.94	0.22	416.22	0.26
22	120.85	0.37	0.51	0.99	0.25	441.96	0.28
23	153.39	0.48	0.62	1.28	0.26	565.83	0.36
24	91.73	0.28	0.37	0.76	0.16	338.35	0.21
25	194.24	0.62	0.80	1.63	0.33	715.18	0.46
26	144.47	0.46	0.59	1.21	0.25	531.69	0.34
27	117.24	0.36	0.45	0.98	0.17	436.08	0.27
28	194.16	0.61	0.79	1.63	0.32	716.71	0.46
29	145.86	0.45	0.61	1.21	0.28	535.43	0.34
30	119.07	0.36	0.48	0.99	0.20	440.23	0.28
31	185.02	0.58	0.75	1.55	0.31	682.00	0.43
32	179.32	0.57	0.69	1.53	0.21	669.03	0.43
33	120.12	0.37	0.48	1.00	0.21	443.27	0.28

Table 3.

Summary of hazard parameters ( $D_{IN}$ ,  $H_{ex}$ ,  $H_{in}$ ,  $I_\gamma$ ,  $I_\alpha$  in sediment samples.

Hazard Parameters	Minimum	Maximum	Mean	Standard Deviation	Median	World average/ recommended value	Increase/ decrease of mean with world average in %
$D_{IN}$ (nGy/h)	89.55	194.24	137.07	30.86	133.95	84	(+) 63.2
$H_{ex}$	0.28	0.62	0.42	0.1	0.4	$\leq 1$	(-) 58
$H_{in}$	0.35	0.8	0.54	0.12	0.5	$\leq 1$	(-) 46
$I_\gamma$	0.74	1.63	1.15	0.27	1.12	$\leq 1$	(+) 15
$I_\alpha$	0.11	0.33	0.21	0.05	0.2	$\leq 1$	(-) 79
AGED ( $\mu$ Sv/y)	330	716.71	508.66	116.24	503.54	300	(+) 70
ELCR $\times 10^{-3}$	0.21	0.46	0.32	0.07	0.31	0.29	(+) 10.34

(+: Increase in value

(-): Decrease in value

Table 4.

Summary of  $^{226}\text{Ra}$ ,  $^{232}\text{Th}$  and  $^{40}\text{K}$  activity concentration ratios.

Ratio	Minimum	Maximum	Mean
$^{226}\text{Ra}/^{232}\text{Th}$	0.38	1.19	0.82
$^{232}\text{Th}/^{226}\text{Ra}$	0.84	2.64	1.34
$^{226}\text{Ra}/^{40}\text{K}$	0.02	0.19	0.1
$^{232}\text{Th}/^{40}\text{K}$	0.05	0.27	0.13

Table 5.

Pearson's correlation coefficient among the variables.

	$^{226}\text{Ra}$	$^{232}\text{Th}$	$^{40}\text{K}$	$D_{IN}$	$H_{ex}$	$H_{in}$	$I_\gamma$	$I_\alpha$	AGDE	ELCR
$^{226}\text{Ra}$	1									
$^{232}\text{Th}$	0.522	1								
$^{40}\text{K}$	-0.422	0.129	1							
$D_{IN}$	0.458	<b>0.918</b>	0.446	1						
$H_{ex}$	0.5	<b>0.948</b>	0.37	<b>0.996</b>	1					
$H_{in}$	0.675	<b>0.937</b>	0.206	<b>0.962</b>	<b>0.976</b>	1				
$I_\gamma$	0.432	<b>0.923</b>	0.455	<b>0.999</b>	<b>0.995</b>	<b>0.955</b>	1			
$I_\alpha$	<b>0.999</b>	0.519	-0.438	0.458	0.499	0.674	0.432	1		
AGDE	0.417	<b>0.909</b>	0.483	<b>0.999</b>	<b>0.992</b>	<b>0.949</b>	<b>0.999</b>	0.417	1	
ELCR	0.422	<b>0.927</b>	0.442	<b>0.999</b>	<b>0.996</b>	<b>0.958</b>	<b>0.999</b>	0.442	<b>0.998</b>	1

Table 6.

Statistical results from the fuzzy  $c$  – means cluster analysis and members of each cluster. Values correspond to centroids of each variable based on hazard parameters.

Group	Variable	No. of Locations	Mean	D.E	Minimum	Maximum	Members	
1	D <sub>IN</sub>	7	183.94	9.31	167.02	194.24	4	
	H <sub>ex</sub>		0.58	0.03	0.52	0.62	10	
	H <sub>in</sub>		0.71	0.07	0.61	0.8	31	
	I <sub>γ</sub>		1.56	0.07	1.43	1.63	32	
	I <sub>α</sub>		0.23	0.08	0.15	0.33	25	
	AGDE		685.65	30.34	628.59	716.71	28	
	ELCR		0.44	0.02	0.4	0.46	1	
2	D <sub>IN</sub>	12	143.37	10	124.99	158.42	29	8
	H <sub>ex</sub>		0.44	0.04	0.38	0.49	26	23
	H <sub>in</sub>		0.55	0.06	0.45	0.63	11	9
	I <sub>γ</sub>		1.2	0.09	1.03	1.34	2	7
	I <sub>α</sub>		0.21	0.05	0.11	0.28	3	6
	AGDE		533.34	35.7	461.78	596.65	19	
	ELCR		0.34	0.03	0.29	0.37	16	
3	D <sub>IN</sub>	14	108.24	13.32	89.55	124.81	5	20
	H <sub>ex</sub>		0.33	0.04	0.28	0.38	13	27
	H <sub>in</sub>		0.44	0.06	0.35	0.51	21	15
	I <sub>γ</sub>		0.9	0.11	0.74	1.03	14	30
	I <sub>α</sub>		0.19	0.03	0.14	0.25	24	22
	AGDE		399.01	49.18	330	460.25	17	33
	ELCR		0.25	0.03	0.21	0.29	12	18

D.E: Differential Evolution

Table 7.

Membership coefficients (in %, rounded) among the groups.

Sample Location	Group1	Group2	Group3		Cluster	Neighbor	Sil_width
4	100	0	0	→	1	2	0.962
10	100	0	0	→	1	2	0.962
31	100	0	0	→	1	2	0.959
32	98	2	0	→	1	2	0.935
25	97	2	1	→	1	2	0.942
28	97	2	1	→	1	2	0.94
1	70	26	4	→	1	2	0.528
29	0	100	0	→	2	3	0.938
26	0	100	0	→	2	3	0.935
11	0	99	0	→	2	3	0.921
2	1	98	1	→	2	1	0.927
3	1	98	1	→	2	3	0.896
19	4	93	3	→	2	1	0.882
16	5	92	3	→	2	1	0.874
6	2	92	6	→	2	3	0.826
8	2	91	7	→	2	3	0.805
23	8	89	4	→	2	1	0.837
9	32	62	6	→	2	1	0.365
7	5	49	46	→	2	3	-0.095
5	0	1	99	→	3	2	0.886
13	1	4	95	→	3	2	0.862
21	1	5	94	→	3	2	0.814
14	2	6	92	→	3	2	0.845
24	2	7	91	→	3	2	0.837
17	2	7	90	→	3	2	0.831
12	3	8	89	→	3	2	0.822
20	2	12	86	→	3	2	0.723
27	3	18	79	→	3	2	0.635
15	3	22	76	→	3	2	0.582
30	3	22	75	→	3	2	0.567
22	3	25	72	→	3	2	0.53
33	3	26	71	→	3	2	0.51
18	5	47	48	→	3	2	0.002

Sil\_width: Silhouette width





Fig. 1. Map of sampling locations.

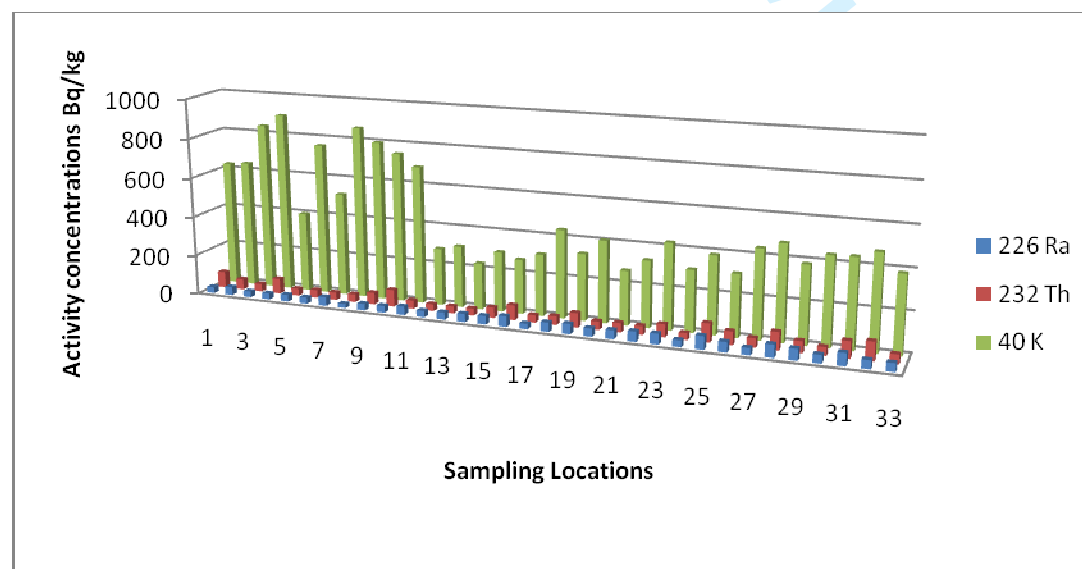


Fig. 2. Activity concentrations of  $^{226}\text{Ra}$ ,  $^{232}\text{Th}$  and  $^{40}\text{K}$  in river sediments along the sampling locations.

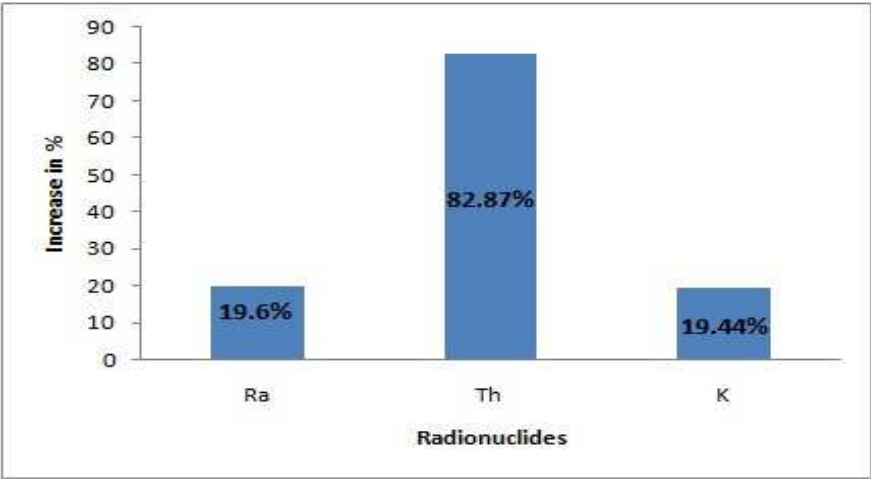
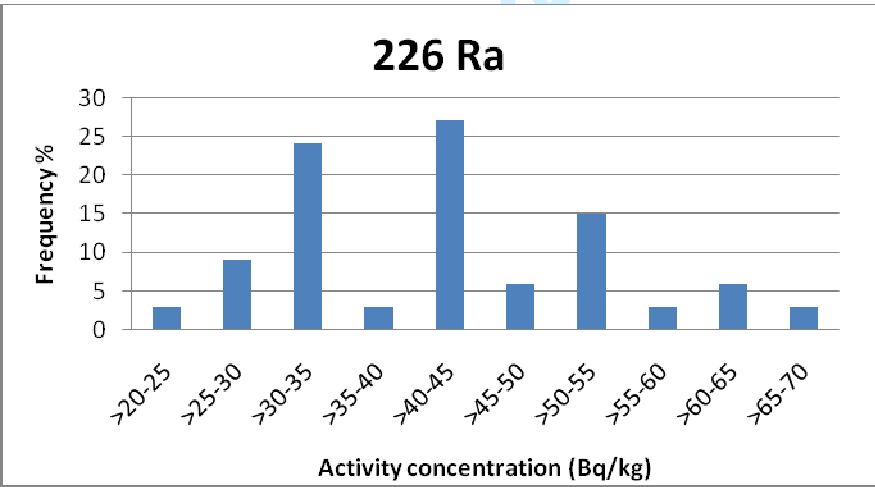


Fig. 3. Increase of natural radionuclides (Bq/kg) in % compared with worldwide mean values



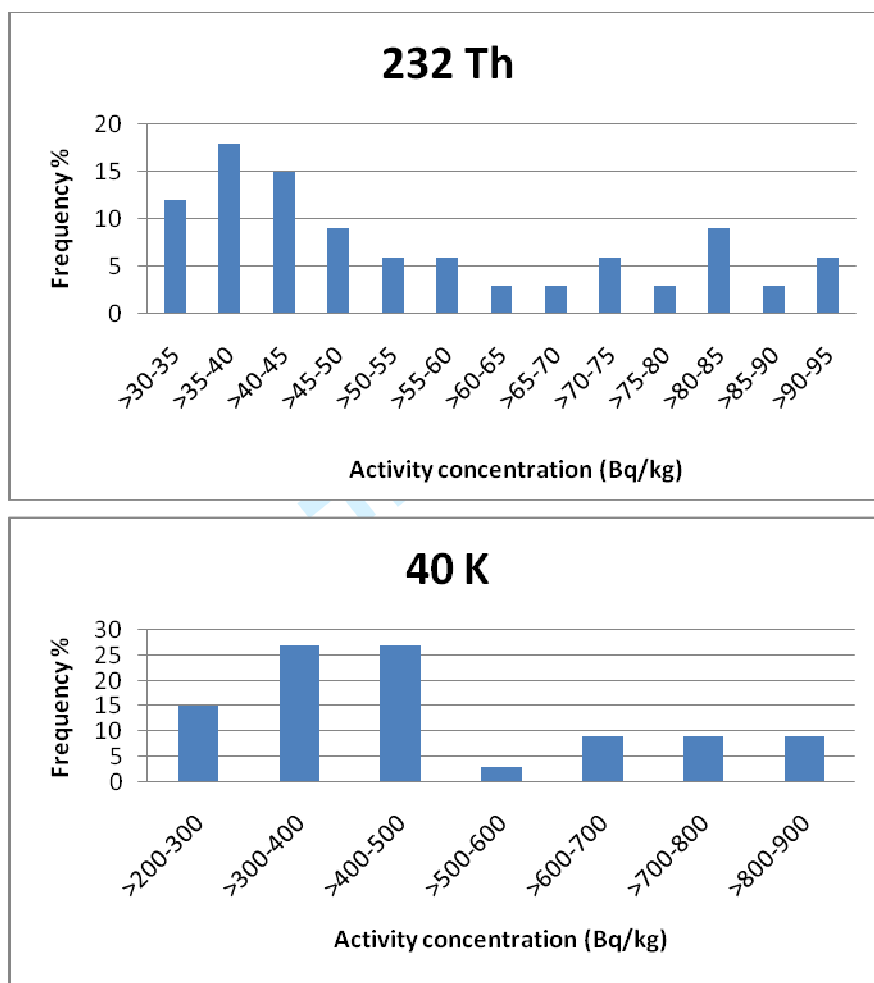


Fig. 4. Frequency distribution of  $^{226}\text{Ra}$ ,  $^{232}\text{Th}$  and  $^{40}\text{K}$  activity concentrations measured in the Bharathapuzha river sediment samples

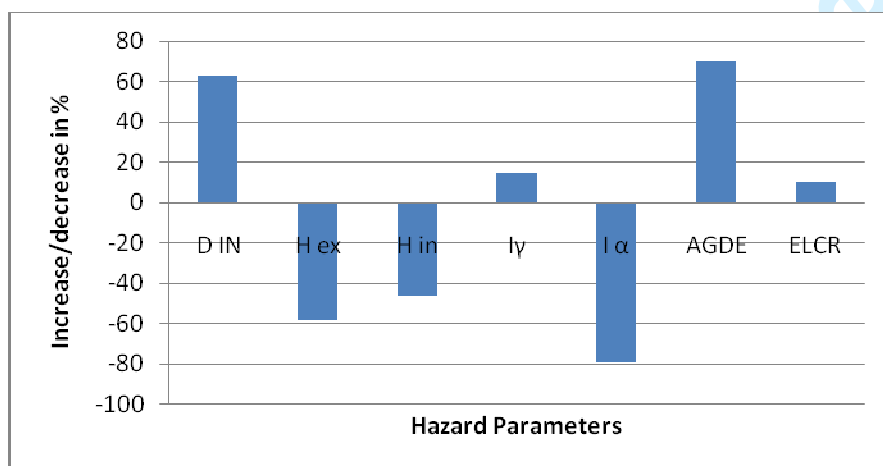


Fig. 5. Increase/decrease % of radiological hazard indices compared with worldwide mean values.

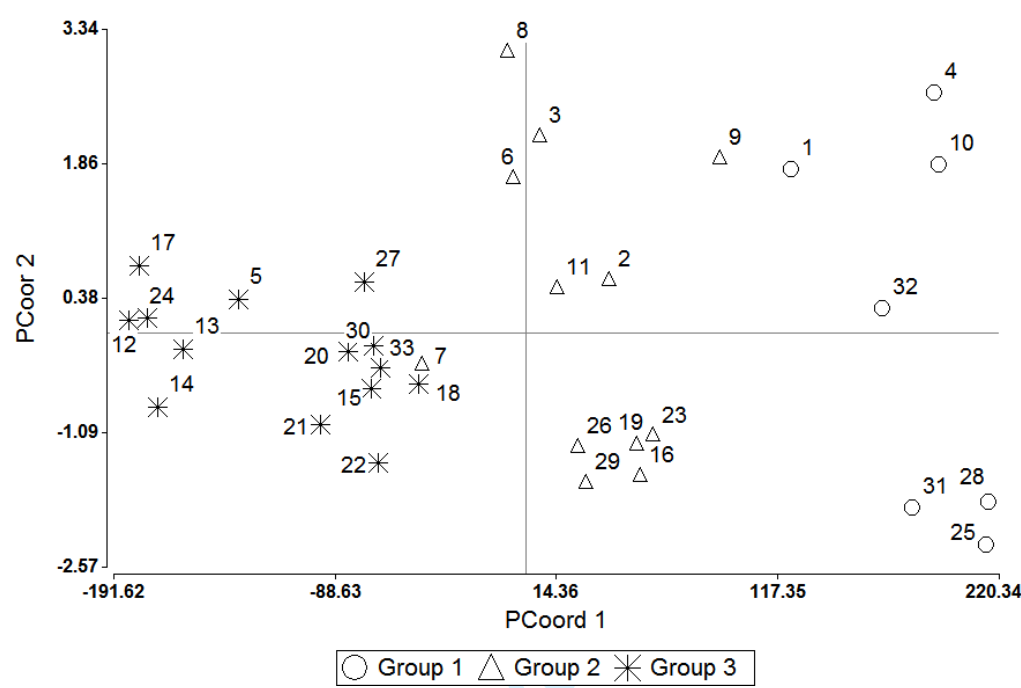


Fig.6. FCC classification, the obtained groups are represented in the coordinate plane (PC 1 and PC 2).

Table 1.

Summary of activity concentrations of  $^{226}\text{Ra}$ ,  $^{232}\text{Th}$  and  $^{40}\text{K}$  in sediment samples.

Radionuclides	Minimum (Bq/kg)	Maximum (Bq/kg)	Mean (Bq/kg)	Standard Deviation	Median	World Average (Bq/kg)	Increase/Decrease of mean with world average in %
$^{226}\text{Ra}$	21.21	66.03	41.86	10.73	40.99	35	(+) 19.6
$^{232}\text{Th}$	33.49	93.1	54.86	19.27	45.96	30	(+) 82.87
$^{40}\text{K}$	232.25	899.66	477.75	192.62	428.03	400	(+) 19.44

(+): Increase in value

Table 2.

Indoor dose rate ( $D_{\text{IN}}$ ) and radiological hazard parameters ( $H_{\text{ex}}$ ,  $H_{\text{in}}$ ,  $I_{\gamma}$ ,  $I_{\alpha}$ , AGED and ELCR) in sediment samples.

Sample Location Number	$D_{\text{IN}}$ (nGy/h)	$H_{\text{ex}}$	$H_{\text{in}}$	$I_{\alpha}$	$I_{\gamma}$	AGED ( $\mu\text{Sv/y}$ )	ELCR ( $\times 10^{-3}$ )
1	167.02	0.52	0.61	1.43	0.15	628.59	0.40
2	146.48	0.45	0.56	1.22	0.20	546.41	0.34
3	136.73	0.40	0.48	1.14	0.15	515.81	0.32
4	183.24	0.56	0.64	1.56	0.15	693.02	0.44
5	102.42	0.31	0.40	0.85	0.17	379.42	0.24
6	133.95	0.40	0.48	1.12	0.16	503.54	0.31
7	124.99	0.38	0.50	1.03	0.23	461.78	0.29
8	131.95	0.39	0.45	1.11	0.11	501.43	0.31
9	158.42	0.48	0.57	1.34	0.16	596.65	0.37
10	184.59	0.58	0.67	1.57	0.17	695.05	0.44
11	140.40	0.42	0.54	1.16	0.21	523.15	0.32
12	89.55	0.28	0.36	0.74	0.16	330.00	0.21
13	96.33	0.30	0.39	0.80	0.18	354.37	0.22
14	94.03	0.29	0.40	0.77	0.20	343.18	0.22
15	119.29	0.37	0.49	0.99	0.21	439.23	0.28
16	152.29	0.49	0.63	1.28	0.26	559.96	0.36
17	90.26	0.28	0.35	0.76	0.14	335.01	0.21
18	124.81	0.38	0.50	1.03	0.23	460.25	0.29
19	151.53	0.48	0.62	1.27	0.25	558.44	0.36
20	116.03	0.36	0.47	0.96	0.20	428.53	0.27
21	113.60	0.36	0.48	0.94	0.22	416.22	0.26
22	120.85	0.37	0.51	0.99	0.25	441.96	0.28
23	153.39	0.48	0.62	1.28	0.26	565.83	0.36
24	91.73	0.28	0.37	0.76	0.16	338.35	0.21

25	194.24	0.62	0.80	1.63	0.33	715.18	0.46
26	144.47	0.46	0.59	1.21	0.25	531.69	0.34
27	117.24	0.36	0.45	0.98	0.17	436.08	0.27
28	194.16	0.61	0.79	1.63	0.32	716.71	0.46
29	145.86	0.45	0.61	1.21	0.28	535.43	0.34
30	119.07	0.36	0.48	0.99	0.20	440.23	0.28
31	185.02	0.58	0.75	1.55	0.31	682.00	0.43
32	179.32	0.57	0.69	1.53	0.21	669.03	0.43
33	120.12	0.37	0.48	1.00	0.21	443.27	0.28

Table 3.

Summary of hazard parameters ( $D_{IN}$ ,  $H_{ex}$ ,  $H_{in}$ ,  $I_{\gamma}$ ,  $I_{\alpha}$  in sediment samples.

Hazard Parameters	Minimum	Maximum	Mean	Standard Deviation	Median	World average/ recommended value	Increase/ decrease of mean with world average in %
$D_{IN}$ (nGy/h)	89.55	194.24	137.07	30.86	133.95	84	(+)63.2
$H_{ex}$	0.28	0.62	0.42	0.1	0.4	$\leq 1$	(-) 58
$H_{in}$	0.35	0.8	0.54	0.12	0.5	$\leq 1$	(-) 46
$I_{\gamma}$	0.74	1.63	1.15	0.27	1.12	$\leq 1$	(+)15
$I_{\alpha}$	0.11	0.33	0.21	0.05	0.2	$\leq 1$	(-)79
AGED ( $\mu$ Sv/y)	330	716.71	508.66	116.24	503.54	300	(+)70
ELCR $\times 10^{-3}$	0.21	0.46	0.32	0.07	0.31	0.29	(+)10.34

(+) : Increase in value

(-) : Decrease in value

Table 4.

Summary of  $^{226}\text{Ra}$ ,  $^{232}\text{Th}$  and  $^{40}\text{K}$  activity concentration ratios.

Ratio	Minimum	Maximum	Mean
$^{226}\text{Ra}/^{232}\text{Th}$	0.38	1.19	0.82
$^{232}\text{Th}/^{226}\text{Ra}$	0.84	2.64	1.34
$^{226}\text{Ra}/^{40}\text{K}$	0.02	0.19	0.1
$^{232}\text{Th}/^{40}\text{K}$	0.05	0.27	0.13

Table 5.

Pearson's correlation coefficient among the variables.

	$^{226}\text{Ra}$	$^{232}\text{Th}$	$^{40}\text{K}$	$D_{\text{IN}}$	$H_{\text{ex}}$	$H_{\text{in}}$	$I_{\gamma}$	$I_{\alpha}$	AGDE	ELCR
$^{226}\text{Ra}$	1									
$^{232}\text{Th}$	0.522	1								
$^{40}\text{K}$	-0.422	0.129	1							
$D_{\text{IN}}$	0.458	<b>0.918</b>	0.446	1						
$H_{\text{ex}}$	0.5	<b>0.948</b>	0.37	<b>0.996</b>	1					
$H_{\text{in}}$	0.675	<b>0.937</b>	0.206	<b>0.962</b>	<b>0.976</b>	1				
$I_{\gamma}$	0.432	<b>0.923</b>	0.455	<b>0.999</b>	<b>0.995</b>	<b>0.955</b>	1			
$I_{\alpha}$	<b>0.999</b>	0.519	-0.438	0.458	0.499	0.674	0.432	1		
AGDE	0.417	<b>0.909</b>	0.483	<b>0.999</b>	<b>0.992</b>	<b>0.949</b>	<b>0.999</b>	0.417	1	
ELCR	0.422	<b>0.927</b>	0.442	<b>0.999</b>	<b>0.996</b>	<b>0.958</b>	<b>0.999</b>	0.442	<b>0.998</b>	1

Table 6.

Statistical results from the fuzzy  $c$  – means cluster analysis and members of each cluster. Values correspond to centroids of each variable based on hazard parameters.

Group	Variable	No. of Locations	Mean	D.E	Minimum	Maximum	Members	
1	$D_{\text{IN}}$	7	183.94	9.31	167.02	194.24	4	
	$H_{\text{ex}}$		0.58	0.03	0.52	0.62	10	
	$H_{\text{in}}$		0.71	0.07	0.61	0.8	31	
	$I_{\gamma}$		1.56	0.07	1.43	1.63	32	
	$I_{\alpha}$		0.23	0.08	0.15	0.33	25	
	AGDE		685.65	30.34	628.59	716.71	28	
	ELCR		0.44	0.02	0.4	0.46	1	
2	$D_{\text{IN}}$	12	143.37	10	124.99	158.42	29	8
	$H_{\text{ex}}$		0.44	0.04	0.38	0.49	26	23
	$H_{\text{in}}$		0.55	0.06	0.45	0.63	11	9
	$I_{\gamma}$		1.2	0.09	1.03	1.34	2	7
	$I_{\alpha}$		0.21	0.05	0.11	0.28	3	6
	AGDE		533.34	35.7	461.78	596.65	19	
	ELCR		0.34	0.03	0.29	0.37	16	
3	$D_{\text{IN}}$	14	108.24	13.32	89.55	124.81	5	20
	$H_{\text{ex}}$		0.33	0.04	0.28	0.38	13	27
	$H_{\text{in}}$		0.44	0.06	0.35	0.51	21	15
	$I_{\gamma}$		0.9	0.11	0.74	1.03	14	30
	$I_{\alpha}$		0.19	0.03	0.14	0.25	24	22
	AGDE		399.01	49.18	330	460.25	17	33
	ELCR		0.25	0.03	0.21	0.29	12	18

D.E: Differential Evolution



Table 7.

Membership coefficients (in %, rounded) among the groups.

Sample Location	Group1	Group2	Group3		Cluster	Neighbor	Sil_width
4	100	0	0	➔	1	2	0.962
10	100	0	0	➔	1	2	0.962
31	100	0	0	➔	1	2	0.959
32	98	2	0	➔	1	2	0.935
25	97	2	1	➔	1	2	0.942
28	97	2	1	➔	1	2	0.94
1	70	26	4	➔	1	2	0.528
29	0	100	0	➔	2	3	0.938
26	0	100	0	➔	2	3	0.935
11	0	99	0	➔	2	3	0.921
2	1	98	1	➔	2	1	0.927
3	1	98	1	➔	2	3	0.896
19	4	93	3	➔	2	1	0.882
16	5	92	3	➔	2	1	0.874
6	2	92	6	➔	2	3	0.826
8	2	91	7	➔	2	3	0.805
23	8	89	4	➔	2	1	0.837
9	32	62	6	➔	2	1	0.365
7	5	49	46	➔	2	3	-0.095
5	0	1	99	➔	3	2	0.886
13	1	4	95	➔	3	2	0.862
21	1	5	94	➔	3	2	0.814
14	2	6	92	➔	3	2	0.845
24	2	7	91	➔	3	2	0.837
17	2	7	90	➔	3	2	0.831
12	3	8	89	➔	3	2	0.822
20	2	12	86	➔	3	2	0.723
27	3	18	79	➔	3	2	0.635
15	3	22	76	➔	3	2	0.582
30	3	22	75	➔	3	2	0.567
22	3	25	72	➔	3	2	0.53
33	3	26	71	➔	3	2	0.51
18	5	47	48	➔	3	2	0.002

Sil\_width: Silhouette width